

Diagnosis and Location of Pinhole Defects in Tunnel Junctions using only Electrical Measurements

Zhongsheng Zhang and David A. Rabson

Department of Physics, PHY 114, University of South Florida, Tampa, FL 33620, USA

Abstract

In the development of the first generation of sensors and memory chips based on spin-dependent tunneling through a thin trilayer, it has become clear that pinhole defects can have a deleterious effect on magnetoresistance. However, current diagnostic protocols based on Andreev reflection and the temperature dependence of junction resistance may not be suitable for production quality control. We show that the current density in a tunnel junction in the cross-strip geometry becomes very inhomogeneous in the presence of a single pinhole, yielding a four-terminal resistance that depends on the location of the pinhole in the junction. Taking advantage of this position dependence, we propose a simple protocol of four four-terminal measurements. Solving an inverse problem, we can diagnose the presence of a pinhole and estimate its position and resistance.

PACS '03: 73.40.Rw, 73.40.Jn, 85.75.Dd, 85.75.Mm

Semiconductor manufacturers are currently developing magnetic-random-access-memory elements^{1–3} based on magnetic tunnel junctions; such junctions separate two ferromagnetic metallic leads by a thin insulating layer,^{4–6} often made by oxidizing a film of Al or other suitable metal. Both because of the thinness of the insulating layer and because of the possibility of inadequate oxidation, “pinhole” defects—direct metal-metal shorts through the nominal insulator—have attracted significant attention.^{7–13} A single pinhole can also be generated in a previously pinhole-free junction carefully through a voltage ramp^{14–17} or, by implication, inadvertently. Generally, the parasitic current through pinholes detracts from a junction’s magnetoresistance,¹⁸ so methods for diagnosing and locating such defects become important during the development of practical devices. Surprisingly, a fit of differential conductance to the Simmons form¹⁹ fails unambiguously to guarantee the absence of pinholes.^{11,20} Surer methods include the use of an integrated superconducting electrode,²⁰ the temperature dependence of device resistance,^{20–22} and surface decoration.^{7,14}

These diagnostics may not be integrated easily into a development or manufacturing process. We therefore propose a very simple test that not only determines the presence of a pinhole with high confidence but also can typically locate the pinhole to within 7% of the junction area and estimate the pinhole resistance. We propose four four-terminal measurements. A discrete three-dimensional resistor model allows us to compute the result of each measurement for an assumed pinhole position; working backward from a set of four experimental measurements to the pinhole position therefore constitutes an inverse problem, to which we demonstrate a solution. Since the method applies to non-magnetic as well as to magnetic tunnel junctions, we shall generally treat the junctions without reference to magnetic properties.

We will consider the common cross-strip geometry of figure 1, consisting of a conducting top strip separated from a perpendicular conducting bottom strip by a thin insulator. The device's four leads are numbered as in the figure. In a typical four-terminal resistance measurement, as shown, current is injected in lead 1 (top strip) and removed through lead 4 (bottom strip), while the voltage is measured between leads 3 and 2. Moodera and collaborators^{23–24} have pointed out that, because a conducting strip is not an isopotential, such a four-terminal measurement will give misleading, sometimes even negative, absolute resistances when the resistance of the insulating layer is comparable to or smaller than those of the upper and lower metals. We generalize their observation for a junction shorted by a single pinhole.

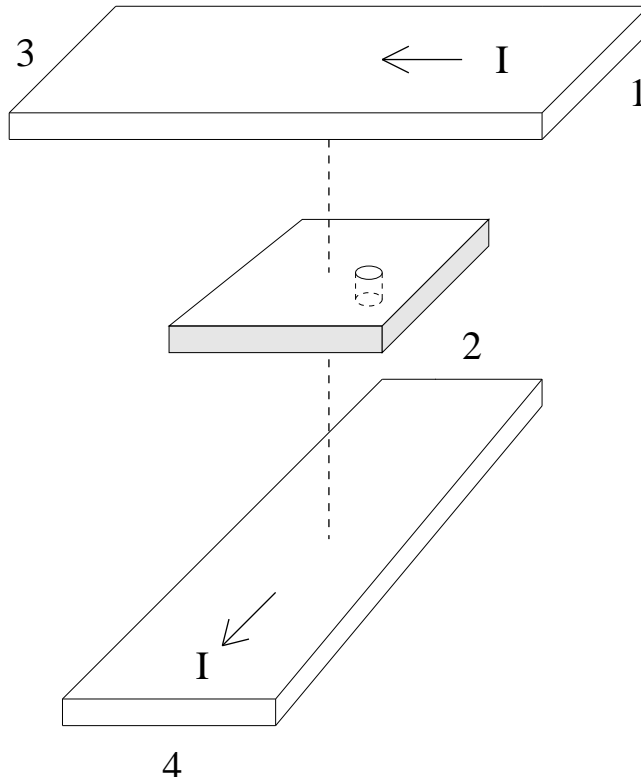


Figure 1. The standard cross-strip geometry (exploded view) consists of a lower metallic strip over which is deposited an aluminum layer, which is oxidized (shaded layer) before a top metallic strip is deposited. To obtain the four-terminal resistance R_1 , one injects current through the leads labeled 1 and 4 while measuring the voltage between leads 3 and 2. A pinhole short through the insulating layer will result in an unreliable four-terminal resistance that depends on the position of the pinhole.

We model the junction as a discretized three-layer resistor network. Each of the four long leads is assumed isopotential where it makes contact with the square junction. (Later, we address this assumption as a source of uncertainty.) The pinhole is modeled as a metallic (Al) inclusion of diameter approximately 0.8 nm penetrating the insulating layer. Classical conductivities are used for conduction through metallic channels, including the pinhole, while the very low conductance of tunneling is approximated from Simmons's formula assuming a barrier height about 2 eV and a thickness around 1 nm. Kirchhoff's law yields a set of linear equations for the potentials at all the nodes of the resistor network in terms of fixed current

I through two leads. We solve the linear equations numerically in order to calculate the voltage difference V between the two measurement leads.

Denote pinhole resistance by R_p and the intrinsic tunnel “resistance,” determined in the Simmons model by the barrier height, area, and thickness, by R_t . Figure 2 plots the nominal four-terminal resistance (R_1) against R_t for R_p fixed at $50\ \Omega$ (horizontal line); the top and bottom layers are given two-dimensional resistivities of $R_{\text{top}} = 10\ \Omega/\square$ and $R_{\text{bot}} = 20\ \Omega/\square$. These values appear representative of recent experiments.^{23–24} The pinhole for this figure was placed in the bottom-left quadrant but not very near the corner. As noted, the nominal four-terminal resistance takes anomalously small, even negative, values when $R_t \ll R_{\text{top}}, R_{\text{bot}}$. The four-terminal measurement is independent of R_t when the latter is large compared to the resistances of the leads, since then most current flows through the pinhole. One thus measures a four-terminal resistance

$$R_1(\mathbf{r}) = R_p + R_{1f}(\mathbf{r}) \quad , \quad (1)$$

where R_{1f} is a function of the pinhole’s position, \mathbf{r} , for fixed R_{top} and R_{bot} . In a junction of sufficiently small area, $R_{\text{top}}, R_{\text{bot}}, R_p \ll R_t$, leaving the positional term, $R_{1f}(\mathbf{r})$, independent of R_p . The inset to figure 2 shows voltage contours on the top layer; the pinhole is evident.

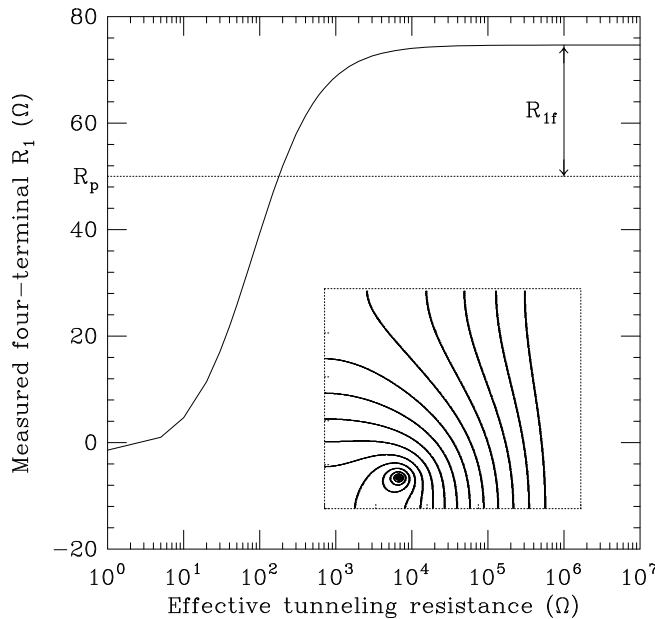


Figure 2. The four-terminal resistance of a junction with a pinhole is plotted as a function of the effective resistance of the tunneling layer. For this illustration, the pinhole resistance $R_p = 50\ \Omega$, while the top- and bottom-layer resistivities take the values $10\ \Omega/\square$ and $20\ \Omega/\square$. When the tunneling resistance is sufficiently large, most of the current flows through the pinhole, and the four-terminal resistance is the sum of the pinhole resistance R_p and a position-dependent piece $R_{1f}(\mathbf{r})$, as in (1). The inset shows constant-voltage contours on the top layer.

We now iterate over all possible pinhole positions, \mathbf{r} . Figure 3 illustrates, for the same parameters as figure 2, the position dependence of $R_1(\mathbf{r})$. If we knew the value of R_p , this figure would localize the pinhole to the curve of constant R_1 corresponding to the measured value.

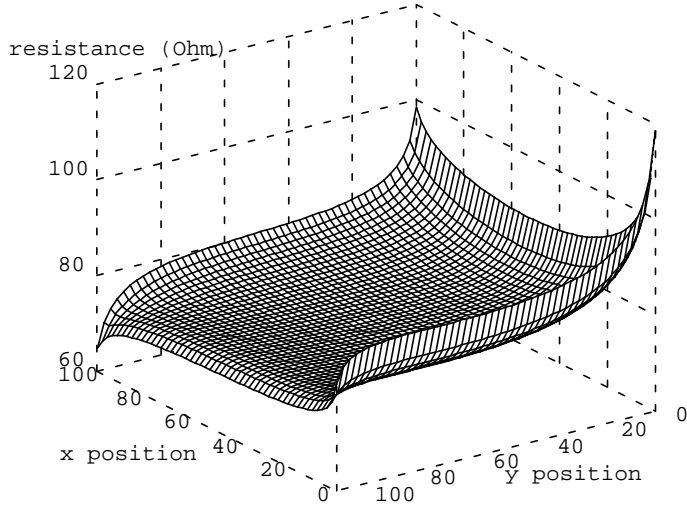


Figure 3. The predicted four-terminal resistance R_1 is plotted against pinhole position. By rotating the roles played by the four leads, one can localize the pinhole over most of the junction area.

In fact, we can find both R_p and \mathbf{r} simply by rotating the roles played by the four electrodes. Thus we measure R_2 by forcing current through leads 1 and 2, measuring voltage across leads 3 and 4. Repeating the rotation, we get four four-terminal measurements, as in table I. In the absence of a pinhole, these four measurements would be equal.

	I	V
R_1	1, 4	3, 2
R_2	2, 1	4, 3
R_3	3, 2	1, 4
R_4	4, 3	2, 1

Table I. Four four-terminal resistances ($R_1 \dots R_4$) are defined from the four ways of injecting current (I) through one top and one bottom lead while measuring the voltage (V) between the remaining two leads.

From (1), differences of the resistances in table I will not depend on the pinhole resistance R_p ; it is convenient²⁵ to take as a maximal independent set

$$\begin{aligned}
 R_a &= R_1 - R_2 + R_3 - R_4 \\
 R_b &= R_1 + R_2 - R_3 - R_4 \\
 R_c &= R_1 - R_2 - R_3 + R_4 \quad .
 \end{aligned}
 \tag{2}$$

Figure 4 displays contour maps of each of the resistances from (2) against position \mathbf{r} of the pinhole, with the contour corresponding to the (simulated) measurement outlined. If we may assume perfect knowledge of the geometry, the three outlined contours will intersect at a point, thus locating the pinhole.

Measurements on an actual tunnel junction will suffer errors and uncertainties from several sources, such as surface roughness and possible non-percolating conducting inclusions. The classical model itself breaks down for junctions small compared to the relevant mean free path. We model the uncertainties in two ways, chosen to be representative rather than microscopically realistic. We then propagate the uncertainties to the calculation of resistances as a function of pinhole position.

First, we consider a break of up to 10% of the junction width at the point where one lead joins the junction, as though there were a bad solder joint. Of course, there is no solder—the strip is continuous—but we use this 10% void as a proxy for uncertainty in the actual junction geometry. A full calculation would find equipotentials bending into the leads where the current is injected rather than coming in straight; inhomogeneity in the leads would further complicate the picture. The 10% void is varied over positions at this junction edge, leading to an error in the four-terminal measurement (compared to the result without the break).

Second, we posit a single atomic-scale terrace in the insulating layer; this too is allowed to migrate over the junction, leading to an error. This source of error stands in as well for possible tunneling “hot spots” due to roughness,^{26–29} so long as the tunnel current remains small compared to the pinhole current. The two sources of uncertainty are combined to give estimated error bars in the resistances R_a , R_b , and R_c . These error bars can be pictured as broadening the outlined contours of figure 4, and the single point of overlap becomes instead a region in which we expect to find the pinhole.

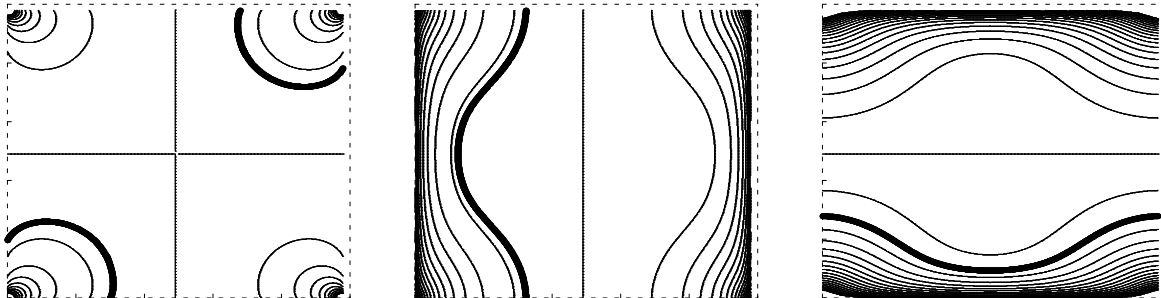


Figure 4. Resistance contours for R_a , R_b , and R_c from equation (2). The resistance that would be measured for the example of figure 2 is emphasized in each. The pinhole is located at the intersection of the three emphasized contours. Because of the two (perpendicular) node lines in R_a , the values are much smaller: the contour scale on R_a is smaller by a factor of 20 than the scales for the other two resistances.

For the sample geometry we have been considering, these sources of error yield uncertainties in each of the four-terminal measurements of 0.5%. If all four measurements R_i (equation (1)) agree within this percentage,³⁰ we conclude with high confidence that the

junction does not harbor a pinhole. (We discuss below the probability of a false negative result.)

We have discussed the calculation of R_i given a known pinhole, but in fact we wish to determine the position of a pinhole given only the measurements R_i . We solve this inverse problem by brute-force computation of four-terminal resistances for all possible positions of a single pinhole on a two-dimensional grid. Confidence regions, as in figure 5, are determined by χ^2 minimization and verified with Monte-Carlo sampling.³¹

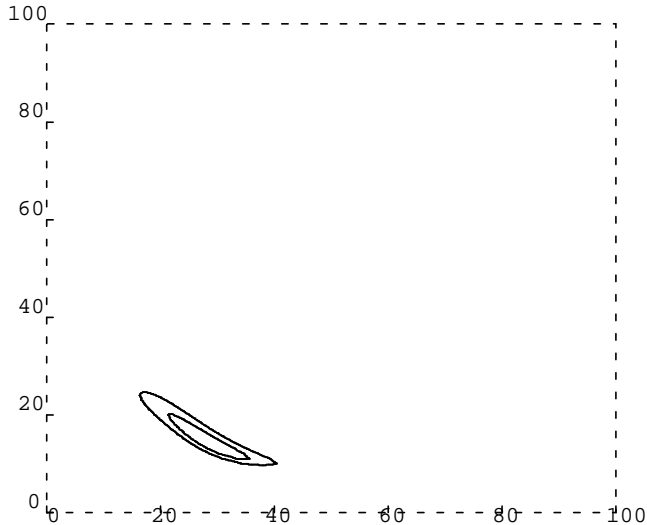


Figure 5. The pinhole of the example localized. The two contours bound 68% and 95% confidence regions as calculated with the χ^2 method. (Monte-Carlo gives similar pictures.)

To extract a confidence region from the χ^2 method, we compare experimental measurements $R_i^{(0)}$ to calculated resistances $R_i(\mathbf{r})$ as functions of pinhole position. The objective function χ^2 is the sum of square errors between calculated and measured resistances, normalized by the estimated variances σ_i^2 :

$$\chi^2(\mathbf{r}) = \sum_{i=a,b,c} \left(\frac{[R_i(\mathbf{r}) - R_i^{(0)}]}{\sigma_i} \right)^2 . \quad (3)$$

We apply the usual chi-square distribution with two degrees of freedom (corresponding to \mathbf{r}) to convert χ^2 contours into confidence regions.

To verify these results with Monte-Carlo sampling, we start with an assumed pinhole position and resistance and calculate the four resistances $R_i^{(0)}$. We then generate a large number of “experimental” data sets $R_i^{(j)}$ by adding Gaussian-distributed noise according to the standard deviations worked out previously. For each data set, we find the pinhole position \mathbf{r} (on the discrete grid) that minimizes χ^2 . With a large number of sets $R_i^{(j)}$, we accumulate the number of times each grid position minimizes the objective function. In the

68% confidence region, we include first the grid point with the largest count, then that with the second-largest count *etc.* until we have included 68% of the data sets. The results agree closely with those from the χ^2 analysis. The procedure could be refined by increasing the number of grid points in the vicinity of the most probable pinhole position until the resolved size fell below the dimensions of the 68% (1-sigma) confidence bound.

We have repeated this calculation for pinhole positions covering the junction area. As the four-fold symmetry makes evident, a pinhole in the very center of the junction would be undetectable through this method, since all four R_i (equation (1)) would be equal. Allowing for estimated errors in the four measurements, we find a region covering about 13% of the area around the center in which a pinhole cannot be distinguished from the absence of a pinhole: a pinhole in this central region still yields measurements R_a, R_b, R_c all equal to zero within an uncertainty 2σ . Confidence regions for pinholes near the central region are larger than for those closer to the edges and corners. Considering all possible actual pinhole positions (including the center), we find that, on average, the 68% confidence region comprises 3.5% of the junction area, while the 95% confidence region comprises 7%. Having located the pinhole, we can solve for R_p in (1) or, to take advantage of averaging, in $R_d = R_1 + R_2 + R_3 + R_4$.

We have proposed a simple technique for diagnosing, with high confidence, the presence or absence of a single pinhole in a tunnel junction and furthermore for determining its position. We hope soon for an experimental test. Pinhole-free junctions may be prepared (and verified using the temperature dependence of resistance^{22,20} or absence of Andreev reflection²⁰) and subjected to the protocol outlined here. The four four-terminal measurements should be equal to within a small uncertainty. To the extent that this uncertainty, derived from a number of junctions, differs from our rough estimate, it will serve to recalibrate our estimated error bars. Then, applying a slow voltage ramp, a single pinhole can be created in each junction. The protocol should determine the pinhole's presence. If possible, it will be interesting to check actual pinhole location with a decoration method^{7,14} or by scanning-probe microscopy.^{26,32}

Work now in preparation investigates the effects of Ohmic heating and thermal transport on the differential conductance of a junction incorporating both a pinhole and tunneling channels. Further work will replace the classical approximations made so far with quantum-mechanical calculations.³³

Acknowledgements

We thank Johan Åkerman for useful comments. DAR is a Cottrell Scholar of Research Corporation, which has supported this work.

References

- ¹ S. Parkin, K. Roche, M. Samant, P. Rice, R. Beyers, R. Scheuerlein, E. O'Sullivan, S. Brown, J. Bucchigano, D. Abraham, Y. Lu, M. Rooks, P. Trouilloud, R. Wanner, and W. Gallagher, *J. Appl. Phys.* **85**, 5828 (1999).
- ² J. M. Daughton, A. V. Pohm, R. T. Fayfield, and C. H. Smith, *J. Phys. D : Appl. Phys.* **32**, R169 (1999).

- ³ W. Reohr, H. Hönigschmid, R. Robertazzi, D. Gogl, F. Pesavento, S. Lammers, K. Lewis, C. Arndt, Y. Lu, H. Viehmann, R. Scheuerlein, L.-K. Wang, P. Trouilloud, S. Parkin, W. Gallagher, and G. Müller, *IEEE Circuits and Devices Magazine* (Sept.), 17 (2002).
- ⁴ M. Jullière, *Phys. Lett.* **54A**, 225 (1975).
- ⁵ T. Miyazaki and N. Tezuka, *J. Magn. Magn. Mat.* **139**, L231 (1995).
- ⁶ J. S. Moodera and G. Mathon, *J. Magn. Magn. Mater.* **200**, 248 (1999).
- ⁷ W. Oepts, H. Verhagen, W. de Jonge, and R. Coehoorn, *Appl. Phys. Lett.* **73**, 2363 (1998).
- ⁸ R. Sousa, J. Sun, V. Soares, P. Freitas, A. Kling, M. da Silva, and J. Soares, *J. Appl. Phys.* **85**, 5258 (1999).
- ⁹ G. Tatara, Y.-W. Zhao, M. Muñoz, and N. García, *Phys. Rev. Lett.* **83**, 2030 (1999).
- ¹⁰ W. Oepts, H. J. Verhagen, R. Coehoorn, and W. J. M. de Jonge, *J. Appl. Phys.* **86**, 3863 (1999).
- ¹¹ B. Jönsson-Åkerman, R. Escudero, C. Leighton, S. Kim, I. K. Schuller, and D. Rabson, *Appl. Phys. Lett.* **77**, 1870 (2000).
- ¹² N. García, *Appl. Phys. Lett.* **77**, 1351 (2000).
- ¹³ D. Rabson, B. Jönsson-Åkerman, A. H. Romero, R. Escudero, C. Leighton, S. Kim, and I. K. Schuller, *J. Appl. Phys.* **89**, 2786 (2001).
- ¹⁴ W. Oepts, H. J. Verhagen, D. de Mooij, V. Zieren, R. Coehoorn, and W. de Jonge, *J. Magn. Magn. Mater.* **198–199**, 164 (1999).
- ¹⁵ K. Shimazawa, N. Kasahara, J. Sun, S. Araki, H. Morita, and M. Matsuzaki, *J. Appl. Phys.* **87**, 5194 (2000).
- ¹⁶ D. Rao, K. Sin, M. Gibbons, S. Funada, M. Mao, C. Chien, and H.-C. Tong, *J. Appl. Phys.* **89**, 7362 (2001).
- ¹⁷ J. Schmalhorst, H. Brückl, M. Justus, A. Thomas, G. Reiss, M. Vieth, G. Gieres, and J. Wecker, *J. Appl. Phys.* **89**, 586 (2001).
- ¹⁸ Reference 12 provides a theoretical mechanism by which pinholes would *not* detract from magnetoresistance, although several experimental investigations (*e.g.*, [8,14,15,16]) *do* see a large effect..
- ¹⁹ J. G. Simmons, *J. Appl. Phys.* **34**, 1793 (1963).
- ²⁰ J. J. Åkerman, R. Escudero, C. Leighton, S. Kim, D. Rabson, R. W. Dave, J. Slaughter, and I. K. Schuller, *J. Magn. Magn. Mater.* **240**, 86 (2002).
- ²¹ J. J. Åkerman, J. Slaughter, R. W. Dave, and I. Schuller, *Appl. Phys. Lett.* **79**, 3104 (2001).
- ²² U. Rüdiger, R. Calarco, U. May, K. Samm, J. Hauch, H. Kittur, M. Sperlich, and G. Güntherodt, *J. Appl. Phys.* **89**, 7573 (2001).

- ²³ J. S. Moodera, L. R. Kinder, J. Nowak, P. Leclair, and R. Meservey, *Appl. Phys. Lett.* **69**, 708 (1996).
- ²⁴ R. van de Veerdonk, J. Nowak, R. Meservey, J. S. Moodera, and W. de Jonge, *Appl. Phys. Lett.* **71**, 2839 (1997).
- ²⁵ The square junction of figure 1 with no pinhole is invariant under the point group D_{2d} ($= \bar{4}2m$), which has a four-dimensional representation on the original measurements R_i , $i = 1\dots 4$. This representation reduces to a one-dimensional non-trivial representation under which R_a is invariant, a two-dimensional representation mixing R_b and R_c , and a trivial one-dimensional representation $R_d = R_1 + R_2 + R_3 + R_4$, only the last of which depends on R_p . Of the other three, only R_a has two nodal lines, meaning that it will generally be small compared to R_b and R_c except in the corners (see figure 4).
- ²⁶ V. Da Costa, F. Bardou, C. Béal, Y. Henry, J. Bucher, and K. Ounadjela, *J. Appl. Phys.* **83**, 6703 (1998).
- ²⁷ Y. Ando, M. Yokota, N. Tezuka, and T. Miyazaki, *J. Magn. Magn. Mat.* **198–199**, 155 (1999).
- ²⁸ J. Buchanan, T. Hase, B. Tanner, N. Hughes, and R. Hicken, *Appl. Phys. Lett.* **81**, 751 (2002).
- ²⁹ L. Dorneles, D. Schaefer, M. Carara, and L. Schelp, *Appl. Phys. Lett.* **82**, 2832 (2003).
- ³⁰ In the combinations (2), the errors are correlated rather than independent, so we apply an error $\sigma = 0.5\%$ instead of twice this value.
- ³¹ W. H. Press, S. A. Teukolsky, W. T. Vetterling, and B. P. Flannery, *Numerical Recipes in C*, Cambridge, 1992.
- ³² W. Wulfhekel, B. Heinrich, M. Klaua, T. Monchesky, F. Zavaliche, R. Urban, and J. Kirschner, unpublished (2000).
- ³³ As an example of a quantum-many-body investigation of a four-terminal measurement, consider S. Hershfield and V. Ambegaokar, *Phys. Rev. B* **38**, 7909 (1989).